

Supplementary Information: Asymmetric Polyoxometalate Electrolytes for Advanced Redox Flow Batteries

Jochen Friedl,^{†,a} Matthäa V. Holland-Cunz,^{†,a} Faye Cording,^a Felix Pfanschilling,^a Corinne Wills,^a William McFarlane,^a Barbara Schricker,^b Robert Fleck,^b Holger Wolfschmidt^b and Ulrich Stimming^{*,a}

^a Chemistry - School of Natural and Environmental Sciences, Bedson Building, Newcastle University, Newcastle upon Tyne, NE1 7RU, United Kingdom

^b Siemens AG, Corporate Technology, 91058 Erlangen, Germany

[†] These authors contributed equally.

1. Materials and Methods

1.1. Synthesis of PV₁₄

All reagents and solvents were purchased from Sigma Aldrich and used without further purification. The hydrated sodium salt of [PV₁₄O₄₂]⁹⁻ (**PV₁₄**), Na_{4.75}H_{4.25}[PV₁₄O₄₂] was obtained by a modification of the preparation by Selling *et al.*¹ The identity of **PV₁₄** was confirmed by dissolving the product in water and taking a ⁵¹V NMR spectrum that showed the three distinct peaks of **PV₁₄**.

Selling *et al.* measured the numbers of protons attached to **PV₁₄** anions in solution by ³¹P and ⁵¹V NMR.¹ They found that there are multiple [H_xPV₁₄O₄₂]^{(9-x)-} species with x = 1-6 in a pH range from 1.5 < pH 6.5. The lower the pH, the higher the number of protons per **PV₁₄** polyoxoanion. As each of the species has its own pK_a value, we assume that **PV₁₄** can act as buffer. Therefore, a titration curve was measured during the formation of **PV₁₄** from NaVO₃ as shown in Fig. S1. Initially, 300g NaVO₃ were dissolved in 1 L of ultra-pure type 1 water (ELGA Option- Q) with 70 mL conc. (85%) phosphoric acid added. Then the pH was measured (Mettler Toledo, Lab 850 benchtop pH meter) while adding concentrated (35%) hydrochloric acid. The protons taken up per **PV₁₄** polyoxoanion *p* were calculated by subtracting the "free protons" *H*_{free}⁺ from the added protons *H*_{added}⁺:

$$H_{\text{added}}^{+} = c_{\text{HCl}} \cdot v \quad (1)$$

$$H_{\text{free}}^{+} = 10^{-\text{pH}} \cdot (v + 1.07\text{L}) \quad (2)$$

$$p = (H_{\text{added}}^{+} - H_{\text{free}}^{+}) / n_{\text{PV}_{14}} \quad (3)$$

With concentration of concentrated (35%) HCl *c*_{HCl} = 12.1 M, volume of added HCl *v*, amount of **PV₁₄** *n*_{PV₁₄} = 0.176 mol.

Fig. S1 shows that the pH of the solution drops from pH 5.8 to pH 2.0 upon addition of 101 mL of concentrated (35%) HCl. The number of protons per **PV₁₄** rises linearly from 0 to 7. The

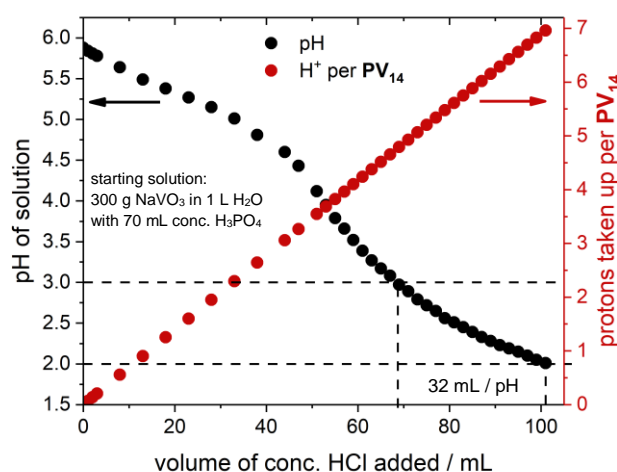


Fig. S1 Titration curve measured during the synthesis of **PV₁₄**. The abscissa gives the volume of added HCl, the left ordinate (black data points) the measured pH values and the right ordinate the calculated number of protons taken up by each **PV₁₄** in solution.

measured pH value exhibits two plateaus during the measurement, indicating that the **PV₁₄** solution acts as a buffer in these regions. Addition of 32 mL of concentrated HCl (35%) changed the pH by one unit, from 3.0 to 2.0.

1.2. ⁵¹V NMR and in-situ NMR

⁵¹V (*I* = 7/2, nat. abund. 99.76%) NMR spectra were measured at 78.94 MHz without proton decoupling on a Bruker Avance III 300 Spectrometer in 5 mm o.d. tubes at a temperature of 298 K. Chemical shifts are relative to neat VOCl₃ as an external reference. 90° excitation pulses of 9.2 μs duration were used, and rapid T₁ relaxation as a result of the nuclear quadrupole led to line widths of 1000 – 2000 Hz. For the in-situ NMR measurements the spectral width was 1188 ppm and the FID was acquired into 1024 data points, leading to an acquisition time of 0.00546 s, so that with a relaxation delay of 0.001 s it was possible to acquire 2048 transients in less than 14 s. Measurements were made at intervals of 85 seconds over a period of 10 hours, and the individual FIDs were transformed

into 32678 points after multiplication by a 50 Hz exponential window.

1.3. Electrochemistry

Three electrode measurements were performed in custom-built glass cells with a polished glassy carbon working electrode (surface area $A = 0.02 \text{ cm}^2$), a gold wire (diameter $d = 0.5 \text{ mm}$) counter electrode and a Mercury/Mercurous Sulfate reference electrode in 1 M H_2SO_4 (MSE, 0.668 V vs. Standard Hydrogen Electrode) (SHE)). Prior to the measurements the electrolyte was purged with nitrogen, and the cell was kept under nitrogen pressure during the experiment. A Bio-Logic SP300 potentiostat was used for control and data acquisition. The flow battery experiments were conducted in a commercial cell (C-Tech 5x5, surface area $A = 25 \text{ cm}^2$). Graphite felts (GFD, SGL Carbon) were used as electrodes and pre-treated at 400°C for 24 h in the laboratory atmosphere. In the cell the 4.6 mm thick electrodes were compressed to 3.5 mm. As membrane a cation exchange membrane (FUMASEP - F1040, thickness $40 \mu\text{m}$) was employed. During the experiment the cell and the pump with tubing were kept in a polycarbonate box purged with nitrogen.

2. Three electrode studies of SiW_{12}

2.1. pH stability of SiW_{12} measured by cyclic voltammetry

pH-stability was assessed by preparing a series of 0.1 M solutions of SiW_{12} and adjusting their pH to values in the range 1 – 6 by addition of 3 M LiOH. These solutions were stored for 24 h and were then diluted to a common pH and concentration (1 mM) by addition of 1 M H_2SO_4 . The CVs are shown in Fig. S2 and indicate that exposure for 24 h to an electrolyte with pH up to 6 does not affect SiW_{12} detrimentally as the CV pattern is very similar for each curve, similar to the CV of freshly prepared SiW_{12} shown in Fig. 1a and is in accord with CV data published in the literature.^{2–4}

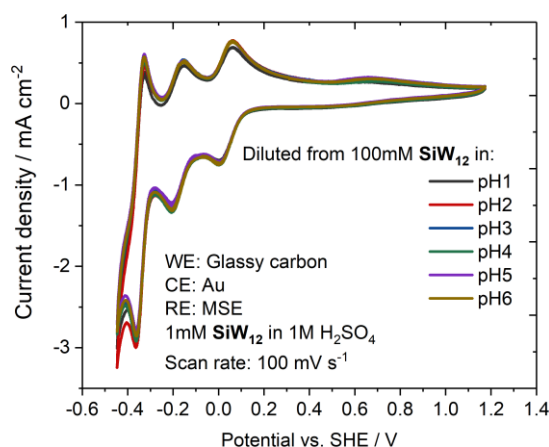


Fig. S2 Cyclic voltammogram of 1 mM SiW_{12} after storage for 24 h in aqueous solution ranging in pH from 1–6. Measured in 1 M H_2SO_4 aqueous solution.

2.2. Electrochemical impedance spectroscopy of SiW_{12}

In order to determine the redox kinetics of SiW_{12} electrochemical impedance spectroscopy (EIS) measurements were performed in a solution with 20 mM SiW_{12} . This solution was reduced by 0.5 electrons per SiW_{12} polyoxoanion by bulk electrolysis. The solution then contained 10 mM SiW_{12} and 10 mM SiW_{12}^{2-} and the measured open circuit potential (OCP) was equal to the measured standard potential of $U_{\text{SiW}_{12}}^{0,1} = 0 \text{ V}$ for the first reduction. EIS was measured at the OCP with an amplitude of 10 mV from 1 MHz to 100 mHz. The obtained spectra were fitted to a Randles Circuit (shown in Fig. S3)

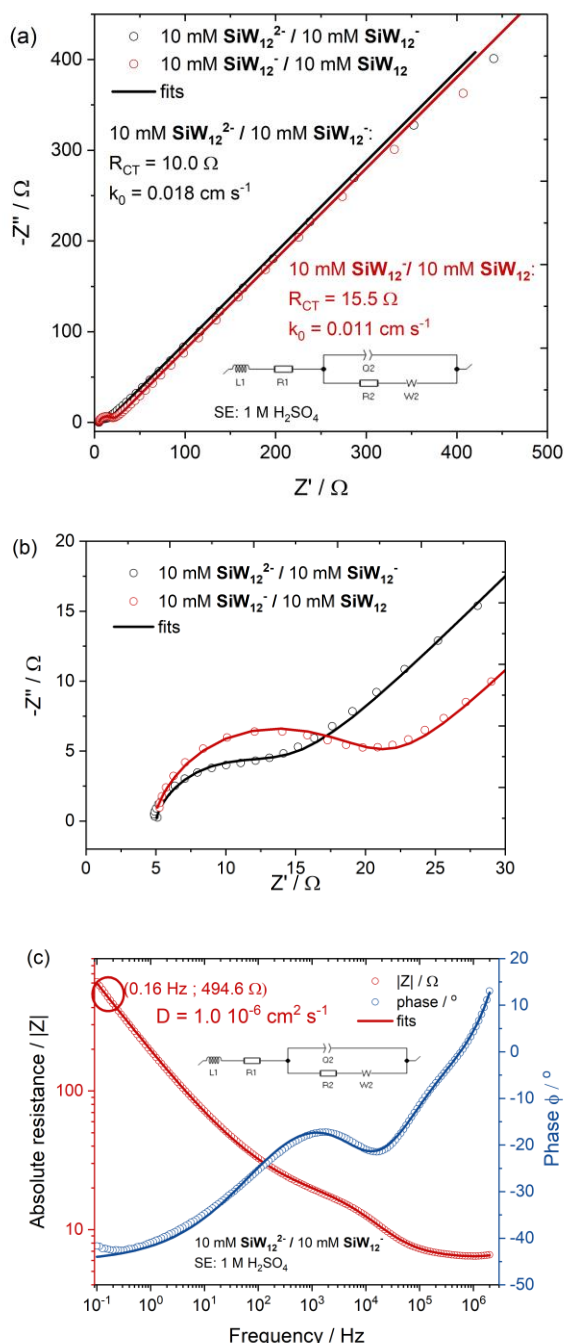


Fig. S3 Electrochemical impedance spectroscopy measurements of the first two redox reactions of SiW_{12} . (a) Nyquist plots of 10 mM $\text{SiW}_{12}^{2-} / 10 \text{ mM } \text{SiW}_{12}^{-}$ and 10 mM $\text{SiW}_{12}^{-} / 10 \text{ mM } \text{SiW}_{12}$ with fits and the used equivalent circuit shown. (b) Detail of (a) showing the semicircle. (c) Bode plot of 10 mM $\text{SiW}_{12}^{2-} / 10 \text{ mM } \text{SiW}_{12}^{-}$ with fits.

Table S1 Parameters for first two redox reactions of **SiW₁₂** determined by fitting the experimental data to the equivalent circuit given in Fig. S3 or by reading the impedance at 0.16 Hz.

	R_{ohm} / Ω	R_{CT} / Ω	$CPE / F s^{(a-1)}$	a	$k_0 / cm s^{-1}$	$C_{DL} / \mu F$	$ Z $ at 0.16 Hz/ Ω	$D / cm^2 s^{-1}$
SiW₁₂/SiW₁₂⁻	4.8	15.5	$2.6 \cdot 10^{-6}$	0.85	0.011	0.31	510	$1.0 \cdot 10^{-6}$
SiW₁₂/SiW₁₂²⁻	4.6	10.0	$21.2 \cdot 10^{-6}$	0.76	0.018	1.0	494	$1.1 \cdot 10^{-6}$

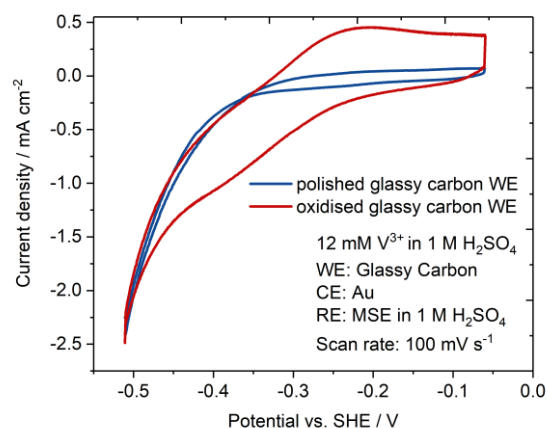
with added inductance accounting for the inductivity of the setup.⁵ The electron transfer constant k_0 was then calculated from the charge transfer resistance R_{CT} obtained from the fit. All fitted parameters are given in Table S1, the double layer capacitance was calculated from the constant phase element (CPE) with the formula given by Hirschorn *et al.* for a surface distribution.⁶ The measurement described above was repeated to measure the kinetics of the second electron transfer of **SiW₁₂**; 1.5 electrons were added to fully oxidised **SiW₁₂**, the composition of the solution is then 10 mM **SiW₁₂⁻** and 10 mM **SiW₁₂²⁻** and the OCP was $U_{SiW_{12}}^{0,2} = -0.21$ V. Nyquist plots for both measurements with their fits are shown in Fig. S3a and S3b. R_{ohm} is very similar for both measurements, the double layer capacitance C_{DL} is lower for **SiW₁₂/SiW₁₂⁻** than for **SiW₁₂/SiW₁₂²⁻**. For the latter measurement a specific capacitance $c_{DL} = 14 \cdot 10^{-6} F cm^{-2}$ is reasonable for a glassy carbon electrode.⁷

The determined electron transfer constants are on the order of $k_0 \approx 10^{-2} cm s^{-1}$. It appears that the second redox reaction **SiW₁₂⁻/SiW₁₂²⁻** is faster than the first redox reaction **SiW₁₂/SiW₁₂⁻**. To the best of our knowledge, this has not been investigated in the literature and could be an interesting research topic.

Diffusion coefficients D can be determined from the magnitude of the admittance ($1/|Z|$) at a frequency of 0.16 Hz (for details see electrochemistry text books such as ref⁸). The calculations yield a very similar diffusion coefficient for **SiW₁₂⁻/SiW₁₂²⁻** and **SiW₁₂/SiW₁₂⁻** at $D = 1.1 \cdot 10^{-6} cm^2 s^{-1}$ and $D = 1.1 \cdot 10^{-6} cm^2 s^{-1}$ respectively. The literature value for D of **[SiW₁₂O₄₀]⁴⁻** in 0.9 M Na₂SO₄, 0.1 M H₂SO₄ at 25 °C is higher at $2.6 \cdot 10^{-6} cm^2 s^{-1}$.³

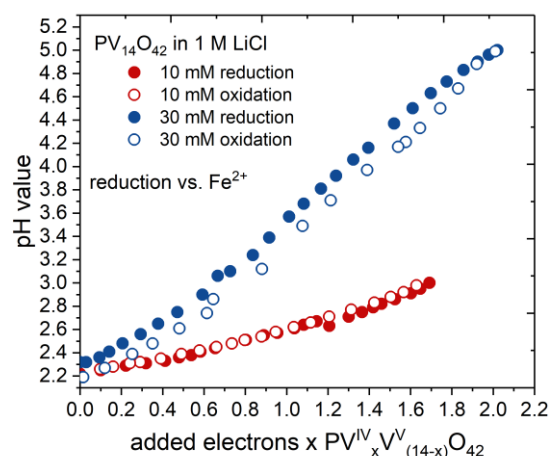
2.3. Cyclic voltammograms of the V²⁺/V³⁺ redox reaction

Fig. 1a in the main manuscript shows a CV of 12 mM V³⁺ on a polished glassy carbon (GC) electrode. The current which is associated with the reduction of V³⁺ and the subsequent reoxidation of V²⁺ is very small, current from the hydrogen evolution reaction appears to be larger. Fig. S4 compares the previously shown CV of 12 mM V³⁺ in 1 M H₂SO₄ on a polished GC electrode with a CV of 12 mM V³⁺ on a GC electrode which has been electrochemically oxidised. For this the potential of the GC electrode was stepped to 2 V vs. SHE for 10 s in 1 M H₂SO₄. The much higher current on the oxidised GC indicates that the electrochemical pretreatment produced a catalytic electrode surface. This is in accordance with other studies that attributed catalytic properties for the V²⁺/V³⁺ redox reaction to oxygen functional groups.^{9–12} The reason for this catalytic effect is most likely a bridge activated electron transfer, as for Fe²⁺/Fe³⁺.^{7,13,14}


Fig. S4 Comparison of the V²⁺/V³⁺ redox reaction on a polished and on an oxidised (2 V vs. SHE for 10 s in 1 M H₂SO₄) glassy carbon working electrode.

3. Investigation of proton coupled electron transfer of PV₁₄

To confirm that the electron transfer of **PV₁₄** is coupled to proton transfer, the polyoxovanadate was reduced and oxidized in a flow battery while the pH was measured in the tank. The other half-cell consisted of an excess of Fe²⁺. The result is shown in Fig. S5. Upon reduction the pH increases, as **PV₁₄** takes up electrons and protons. This behaviour is reversible, and depends on the concentration of **PV₁₄** as expected.


Fig. S5 Evolution of pH value during reduction and oxidation of **PV₁₄** against an excess of Fe²⁺. The measurement is shown for two concentrations: 10 mM (red circles) and 30 mM (blue circles) **PV₁₄** for reduction and oxidation.

4. ^{51}V NMR investigation of PV_{14} to measure pH stability

The pH stability of PV_{14} was measured by ^{51}V NMR. For this purpose spectra in electrolytes ranging in pH from 1.1 to 2.1 were recorded immediately after adjusting the pH, and again after 3, 6 and 78 hours. The ratio of free vanadium (VO_2^+) to PV_{14} was determined by integrating the intensities of the peaks labelled PV_{14}^3 and VO_2^+ . The signal PV_{14}^3 arises from two vanadium sites in PV_{14} , and so its integrated intensity was divided by 2 for comparison with the single vanadium site in VO_2^+ .

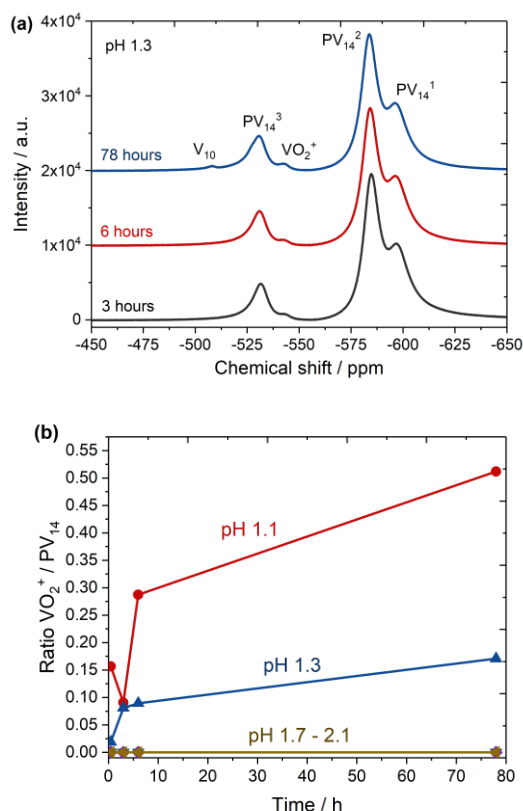


Fig. S6 (a) Typical ^{51}V NMR spectra for 50 mM PV_{14} in water with pH 1.3: 3 hours after adjusting the pH (black curve), after 6 hours (red curve) and after 78 hours (blue curve). (b) Development of VO_2^+ to PV_{14} ratio evaluated over time. The three lines for pH 1.7, 1.9 and 2.1 overlap.

5. Battery studies

The cross-over studies were performed by separating two half-cells each with a volume of 32 cm³ by a membrane with a surface area of 16 cm². One of the half-cells contained a concentration c of 100 mM of the species under investigation (Fe^{2+} or SiW_{12}) in 1 M H_2SO_4 , the electrolyte in the other half-cell was $c = 20$ mM of V^{3+} in the case of Fe^{2+} and $c = 20$ mM of Fe^{2+} in the case of SiW_{12} . The half-cell with the high concentration was stirred. In the half-cell with the lower concentration a working-, counter- and reference electrode were used to measure CVs periodically. The measured peak currents for Fe^{2+} and SiW_{12} were then converted to concentrations and plotted as seen in Fig. S7.

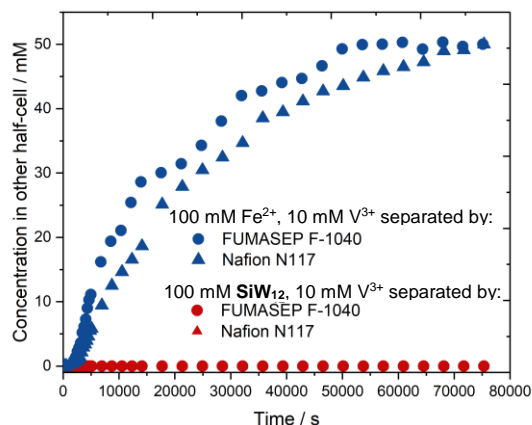


Fig. S7 Time dependent concentration of Fe^{2+} (blue data) and SiW_{12} (red data) measured by CVs in a half-cell that did not contain these species at $t = 0$ s.

Electrochemical impedance spectroscopy was employed at an open circuit voltage of 1 V with an amplitude of 10 mV and in a frequency range $10 \text{ kHz} \leq f \leq 50 \text{ mHz}$. The resulting Nyquist plot is shown in Fig. S8.

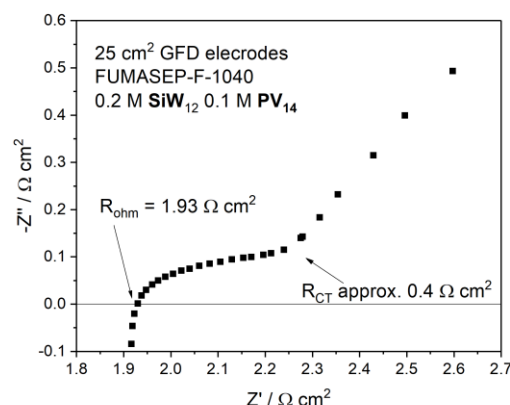


Fig. S8 Nyquist spectrum of the flow cell after 155 cycles at an open circuit voltage of 1 V with values for R_{ohm} and R_{CT} given.

A ^{51}V NMR spectrum of the catholyte was obtained after the 155 charge and discharge cycles shown in Fig. 5 at a moment when it was fully charged. The pH of the solution was 1.2. This spectrum is shown in Fig. S9 and is very similar to the spectra shown in Fig. S6a. Most of the vanadium is present as PV_{14} , however, a contribution from VO_2^+ at -544 ppm is also visible. Fitting of the peaks and data analysis revealed that the ratio of VO_2^+ to PV_{14}^3 signals is 0.10, and therefore the presence of VO_2^+ is as expected for the measured pH. This indicates, that degradation due to electrochemical processes does not contribute to the decomposition of PV_{14} . A ^{51}V NMR spectrum of the anolyte after 155 charge and discharge cycles gave no signal, indicating that no vanadium containing species had crossed through the membrane.

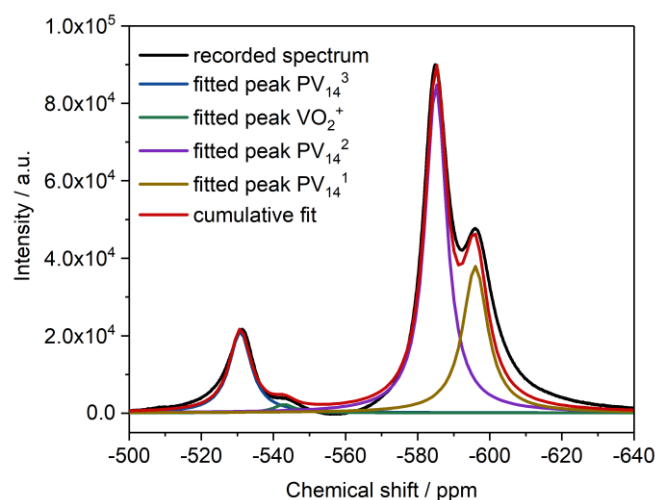


Fig. S9 ^{51}V NMR spectra of the catholyte after 155 charge and discharge cycles which took 14 days. The individual contributions were fitted to Lorentzian curves.

Table S2. Peak positions and integrated intensities for the curves fitted to the ^{51}V spectrum shown in Fig. S9.

Peak	Chemical shift / ppm	Integrated Intensity	Ratio to PV_{14}^3
PV_{14}^3	-530.8	240000	1
VO_2^+	-543.0	23500	0.10
PV_{14}^2	-585.1	960000	4.0
PV_{14}^1	-596.0	495000	2.1

Bibliography

- Selling, A.; Andersson, I.; Pettersson, L.; Schramm, C. M.; Downey, S. L.; Grate, J. H. *Inorg. Chem.* **1994**, 33 (13), 3141–3150.
- Sadakane, M.; Steckhan, E. *Chem. Rev.* **1998**, 98 (1), 219–238.
- Pope, M.; Varga, G. M. *Inorg. Chem.* **1966**, 5 (7), 3–8.
- Keita, B.; Nadjo, L. *J. Electroanal. Chem. Interfacial Electrochem.* **1987**, 227 (1–2), 77–98.
- Friedl, J.; Stimming, U. *Electrochim. Acta* **2017**, 227, 235–245.
- Hirschorn, B.; Orazem, M. E.; Tribollet, B.; Vivier, V.; Frateur, I.; Musiani, M. *Electrochim. Acta* **2010**, 55 (21), 6218–6227.
- McCreery, R. L. *Carbon N. Y.* **2008**, 108 (7), 2646–2687.
- Bard, A.; Faulkner, L. *Electrochemical methods: Fundamentals and Applications*, Second.; Harris, D., Swain, E., Robey, C., Aiello, E., Eds.; John Wiley and Sons: New York, 2001.
- Miller, M. A.; Bourke, A.; Quill, N.; Wainright, J. S.; Lynch, R. P.; Buckley, D. N.; Savinell, R. F. *J. Electrochem. Soc.* **2016**, 163 (9), A2095–A2102.
- Bourke, A.; Quill, N.; Lynch, R. P.; Buckley, D. N. *ECS Trans.* **2014**, 61 (37), 15–26.
- Bourke, A.; Lynch, R. P.; Buckley, D. N. *ECS Trans.* **2013**, 53 (30), 59–67.
- Fink, H.; Friedl, J.; Stimming, U. *J. Phys. Chem. C* **2016**, 120 (29), 15893–15901.
- Nagy, Z.; Hung, N. C.; Yonco, R. M. *J. Electrochem. Soc.* **1989**, 136 (3), 895.
- Hung, N. G.; Nagy, Z. *J. Electrochem. Soc.* **1987**, 134 (9), 2215–2220.